

Axion effects on quark matter and quark-matter cores in massive hybrid stars

He Liu,^{1,2,*} Yu-Heng Liu,^{1,2} Yong-Hang Yang,^{1,2} Min Ju,^{3,†}
 Xu-Hao Wu,^{4,‡} Hong-Ming Liu,^{1,2,§} and Peng-Cheng Chu^{1,2,¶}

¹Science School, Qingdao University of Technology, Qingdao 266000, China

²The Research Center of Theoretical Physics, Qingdao University of Technology, Qingdao 266033, China

³School of Science, China University of Petroleum (East China), Qingdao 266580, China

⁴School of Science, Yanshan University, Qinhuangdao 066004, China

(Dated: December 24, 2024)

Using a three-flavor Nambu–Jona-Lasinio model to describe the charge-parity violating effects through axion field, we investigate the axion effects on quark matter and quark-matter cores in massive hybrid stars. The properties of quark matter vary with the scaled axion field a/f_a in a periodic manner, with a period of 2π . Within the range from 0 to π , axion field decrease the baryon chemical potential of the first-order phase transition, leading to an increase in normalized pressure and stiffening of the quark matter equation of state. The effect of axions on hybrid star matter that includes the hadron-quark phase transition is contrary to expectations. The axion field shifts the onset of the hadron-quark mixed phase to lower densities but slightly softens the equation of state of the mixed phase matter, which also results in a slight decrease in the maximum mass and corresponding radius of the hybrid stars. However, we also find that the lowering of the onset of the mixed phase significantly increases the radius and mass of the quark-matter core in the hybrid star. Therefore, our results indicate with axion effects, a sizable quark-matter core can appear in $2M_\odot$ massive neutron stars.

Introduction. Recent inspiring progress has been made in astrophysical observations on neutron stars (NSs), including the measurements of masses and radii of the millisecond pulsars PSR J0030+0451 [1, 2] and PSR J0740+6620 [3–5] using the Neutron Star Interior Composition Explorer (NICER), as well as the multimessenger observations of gravitational-wave events GW170817 [6] and GW190814 [7] by the LIGO/Virgo Collaboration. These observations of massive neutron stars have advanced our understanding of the equation of state (EOS) for dense, strongly interacting matter. It is generally believed that a first-order phase transition from hadronic matter to quark matter at high baryon densities may occur in the interior of neutron stars (NSs) [8, 9]. Some recent studies, for instance, have also shown that quark-matter core can appear in massive NS [10], and the presence of a first-order phase transition from hadronic to quark matter can imprint signatures in binary NS merger observations [11–13]. The binary NS merger events have recently emerged as a new tool for probing the beyond-the-standard-model (BSM) particles, such as axions and axionlike particles (ALPs) [14–17], CP-even scalars [18], and dark photons [19]. The hot and dense matter in a binary NS merger remnant would efficiently produce ALPs coupling to photons. However, as candidate for cold dark matter [20–22], axions was originally introduced to explain the violation of combined symmetries of charge conjugation and parity (CP violation) in quantum chromo-

dynamics (QCD) [20, 21], which have also been associated with the stellar evolution [24, 25] and the anomalous stellar cooling problem [26, 27]. Hence, this new/exotic matter state would also be produced in the cold constituent NSs before they merge and affect their properties.

Methods. Due to the non-Abelian nature of the gauge fields, QCD allows the topologically nontrivial Chern-Simons term $\mathcal{L}_\theta \sim \theta \text{Tr} G_{\mu\nu} \tilde{G}^{\mu\nu}$. This term has important quantum mechanical consequences, as it leads to an explicit breaking of the CP symmetry in QCD for a non-vanishing value θ [28]. The axion as a pseudo-Goldstone boson from spontaneous breaking of the Peccei-Quinn (PQ) symmetry [29, 30] is an elegant mechanism to solve the strong CP violating problem. The properties of QCD axion, that is, mass and self-coupling, in a hot and dense medium have recently been studied in the framework of the three-flavor Nambu–Jona-Lasinio (NJL) model for quark matter [33, 41, 42]. NJL model as an effective theory has been extensively used to describe chiral symmetry breaking in strong interactions. The CP violating effects through the axion field can be included in the Kobayashi-Maskawa-t’ Hooft (KMT) determinant term [34]. Thus, the Lagrangian density of the three flavor NJL model with axion fields can be given by

$$\begin{aligned} \mathcal{L} = & \bar{\psi}(i\partial\!\!\!/ - \hat{m})\psi + \frac{G_S}{2} \sum_{a=0}^8 [(\bar{\psi}\lambda_a\psi)^2 + (\bar{\psi}i\gamma_5\lambda_a\psi)^2] \\ & - K \{ e^{i\frac{\theta}{f_a}} \det[\bar{\psi}(1 + \gamma_5)\psi] + e^{-i\frac{\theta}{f_a}} \det[\bar{\psi}(1 - \gamma_5)\psi] \} \\ & - \frac{G_V}{2} \sum_{a=0}^8 [(\bar{\psi}\gamma_\mu\lambda_a\psi)^2 + (\bar{\psi}\gamma_5\gamma_\mu\lambda_a\psi)^2], \end{aligned} \quad (1)$$

where $\psi = (u, d, s)^T$ represents the quark field with three flavors, $\hat{m} = \text{diag}(m_u, m_d, m_s)$ is the current quark mass matrix, and λ_a shows the flavor SU(3) Gell-Mann matrices.

* liuhe@qut.edu.cn

† jumin@upc.edu.cn

‡ wuhaoyu@ysu.edu.cn

§ liuhongming13@126.com

¶ kyois@126.com

ces with $\lambda_0 = \sqrt{2/3}I$. G_S and G_V are, respectively, the scalar and vector coupling constants. The K term in Eq. (1) represents the six-point interaction that breaks the axial symmetry $U(1)_A$ [34]. The normalized axion field in the term K is denoted as $a(x) = \theta(x)f_a$, where f_a is the decay constant of the axion which also represents the PQ symmetry breaking scale. The properties of the axion are controlled by the decay constant of the axion f_a . Astrophysical observations, e.g., cooling rate of the SN1987A supernova and black hole superradiance, put stringent constraint on the PQ symmetry-breaking scale with $10^8 \leq f_a \leq 10^{17}$ GeV [35–37]. Typically, one could consider f_a to be of the order of the grand unified scale $\sim 10^{16}$ GeV. In our case, we are dealing with a much smaller energy scale than the axion symmetry-breaking energy. Hence, we can take the axion field a to be in its vacuum expectation value, and the interaction between the axion field and the QCD gauge field now can be expressed as $\mathcal{L}_\theta \sim (a/f_a)\text{Tr}G_{\mu\nu}G^{\mu\nu}$.

In the mean-field approximation, the thermodynamic potential from the finite-temperature field theory can be expressed as

$$\begin{aligned} \Omega = & -2N_c \sum_i \left\{ \int_0^\Lambda \frac{d^3p}{(2\pi)^3} E_i + \int \frac{d^3p}{(2\pi)^3} [T \ln(1 + e^{-\beta(E_i - \tilde{\mu}_i)}) \right. \\ & + T \ln(1 + e^{-\beta(E_i + \tilde{\mu}_i)})] \left. \right\} + \sum_i [G_S(\sigma_i^2 + \eta_i^2) - G_V \rho_i^2] \\ & - 4K \left[\cos \frac{a}{f_a} (\sigma_u \sigma_d \sigma_s - \sigma_s \eta_u \eta_d - \sigma_u \eta_d \eta_s - \sigma_d \eta_u \eta_s) \right. \\ & \left. - \sin \frac{a}{f_a} (\eta_u \eta_d \eta_s - \sigma_u \sigma_s \eta_d - \sigma_d \sigma_s \eta_u - \sigma_u \sigma_d \eta_s) \right], \quad (2) \end{aligned}$$

where the factor $2N_c = 6$ represents the spin and color degeneracy of the quark, $\beta = 1/T$ is the inverse of the temperature, and $\tilde{\mu}_i = \mu_i - 2G_V \rho_i$ is the effective chemical potential. Note that the first integral, corresponding to the vacuum contribution, is ultraviolet divergence, necessitating a cutoff Λ to regularize the three-momentum integration. In contrast, the thermal integrals are finite and have no need for the cutoff [38]. Importantly, the effective number of quark degrees of freedom approaches the correct asymptotic behavior at high temperatures (the Stefan-Boltzmann limit) only when the cutoff is removed from the finite thermal contributions [39]. In the above, $E_i = \sqrt{M_i^2 + p^2}$ with $M_i = \sqrt{M_i^s{}^2 + M_i^p{}^2}$ is the single-particle energy for i -flavor quark, where M_i^s and M_i^p are the scalar and pseudoscalar contributions of the constituent mass given by the gap equations

$$\begin{aligned} M_i^s = & m_i + 2G_S \sigma_i + 2K \left[\cos \frac{a}{f_a} (\sigma_j \sigma_k - \eta_j \eta_k) \right. \\ & \left. + \sin \frac{a}{f_a} (\sigma_j \eta_k + \eta_j \sigma_k) \right], \quad (3) \end{aligned}$$

$$\begin{aligned} M_i^p = & 2G_S \eta_i + 2K \left[\cos \frac{a}{f_a} (\eta_j \sigma_k + \sigma_j \eta_k) \right. \\ & \left. + \sin \frac{a}{f_a} (\eta_j \eta_k - \sigma_j \sigma_k) \right] \quad (4) \end{aligned}$$

with $(i, j, k) = (u, d, s)$. $\sigma_i = \langle \bar{\psi}_i \psi_i \rangle$ and $\eta_i = \langle \bar{\psi}_i i \gamma_5 \psi_i \rangle$ represent scalar and pseudoscalar condensates, respec-

tively. In the case of unbroken isospin symmetry, only nonzero σ_i and/or η_i can arise. When $a/f_a \neq 0$, a nonzero η_i signals that CP invariance is broken, and thus it can serve as an order parameter for the CP-violating phase [40]. Those two condensates can be obtained as [40–42]

$$\sigma_i = -2N_c \left[\int_0^\Lambda \frac{d^3p}{(2\pi)^3} \frac{M_i^s}{E_i} - \int \frac{d^3p}{(2\pi)^3} \frac{M_i^s}{E_i} (f_i + \bar{f}_i) \right] \quad (5)$$

$$\eta_i = 2N_c \left[\int_0^\Lambda \frac{d^3p}{(2\pi)^3} \frac{M_i^p}{E_i} - \int \frac{d^3p}{(2\pi)^3} \frac{M_i^p}{E_i} (f_i + \bar{f}_i) \right], \quad (6)$$

where f_i and \bar{f}_i are respectively the Fermi distribution functions of particle and antiparticle. The pressure and energy density can be derived using the thermodynamic relations in the grand canonical ensemble as $P = -(\Omega - \Omega_0)$ and $\varepsilon = \sum_i \mu_i \rho_i - P$, where Ω_0 is introduced to ensure that the pressure and energy density vanish in the vacuum. In the present study, we employ the parameters $m_u = m_d = 3.6$ MeV, $m_s = 87$ MeV, $G_S \Lambda^2 = 3.6$, $K \Lambda^5 = 8.9$, and the cutoff value in the momentum integral $\Lambda = 750$ MeV given in Refs. [43, 44].

Witten hypothesis suggests that absolutely stable strange quark matter (SQM) might be the true ground state of the strongly interacting matter, which requires the minimum energy per baryon (E/A) of SQM at zero temperature should be less than the minimum energy per baryon of the observed most stable nuclei $M(^{56}\text{Fe})/56 = 930$ MeV [45, 46]. Therefore, it may be a significant challenge to have a quark star composed of pure strange quark matter with an equation of state that is sufficiently stiff to support a massive compact star. To investigate the effects of axions on quark matter in the massive neutron stars, we therefore primarily focus on hybrid stars with the hadron-quark phase transition. We describe nuclear matter using an improved isospin- and momentum-dependent interaction (ImMDI) model. In our previous study [47–49], the ImMDI model is constructed from fitting the properties of cold symmetric nuclear matter (SNM), which is approximately reproduced by the self-consistent Greens function (SCGF) approach [50, 51] or chiral effective many-body perturbation theory (χ EMBPT) [52, 53]. The ImMDI model has been extensively used in intermediate energy heavy-ion reactions to study the properties of asymmetric nuclear matter. In ImMDI model, we introduce the parameters x , y and z to adjust the slope L of symmetry energy, the momentum dependence of the symmetry potential, and the symmetry energy E_{sym} at saturation density, respectively. In order to better focus on axion effects on the properties of quark matter in hybrid stars, we thus choose for the hadronic phase a fixed parameter set in ImMDI model, $x = -0.3$, $y = 32$ MeV, and $z = 0$, that would allow $2.08M_\odot$ neutron stars and still satisfy well nuclear matter constraints at saturation density ρ_0 , i.e., the binding energy $E_0(\rho_0) = -15.9$ MeV, the incompressibility $K_0 = 240$ MeV, the symmetry energy $E_{sym}(\rho_0) = 32.5$ MeV, the slope parameter $L = 106$ MeV, the isoscalar

effective mass $m_s^* = 0.7m$, and the single-particle potential $U_{0,\infty} = 75$ MeV at infinitely large nucleon momentum [49]. In this work, the hadron-quark mixed phase is described by the Gibbs construction [54, 55]: $T^H = T^Q$, $P^H = P^Q$, $\mu_B^H = \mu_B^Q$, and $\mu_c^H = \mu_c^Q$, where μ_B and μ_c are the baryon and charge chemical potential, as well as the labels H and Q represent the hadronic and quark phases, respectively. Including β -equilibrium, baryon number conservation and charge neutrality conditions, the dense matter enters the mixed phase, in which the nuclear and quark matter need to satisfy following equilibrium conditions:

$$\mu_i = \mu_B b_i - \mu_c q_i, \quad (7)$$

$$\rho_B = (1 - Y)(\rho_n + \rho_p) + \frac{Y}{3}(\rho_u + \rho_d + \rho_s), \quad (8)$$

$$0 = (1 - Y)\rho_p + \frac{Y}{3}(2\rho_u - \rho_d - \rho_s) - \rho_e - \rho_\mu, \quad (9)$$

where Y is the baryon number fraction of the quark phase. In fact, for $Y = 0$, the equilibrium conditions can be used to describe a pure hadronic phase, while for $Y = 1$, they can be used to describe a pure quark phase. The crust of hybrid stars, in our calculations, is considered to be divided into two parts: the inner and the outer crust as in the previous treatment [56, 57]. The polytropic form $P = a + b\varepsilon^{4/3}$ has been found to be a good approximation to the inner crust EOS [58], and the outer crust usually consists of heavy nuclei and electron gas, where we use the EOS in Ref. [59]. Using the whole EOS from hadronic to quark phase, the mass-radius relation of hybrid stars can be obtained by solving the Tolman-Oppenheimer-Volkoff (TOV) equation [60].

Results and discussions. We first display in Fig. 1 the axion effects on properties of quark matter at zero temperature from the NJL model with $G_V = 0$. In the present computation, we assume isospin symmetry and set $\mu_u = \mu_d = \mu_s = 1/3\mu_B$, thus ensuring that the properties of up quarks and down quarks among the light quarks are consistent. In Fig. 1(a), we show the baryon chemical potential dependence of contributions to the constituent mass of up quark from the scalar and the pseudoscalar condensates for varying values of the scaled axion field a/f_a . It can be clearly seen that within the range of 0 to π for a/f_a , the scalar mass M_u^s decreases as a/f_a increases, while the absolute value of the pseudoscalar mass M_u^p increases with a/f_a . This forms a complementary relationship, resulting in the total constituent mass $M_u = \sqrt{M_u^s{}^2 + M_u^p{}^2}$ remaining approximately constant for different values of a/f_a . For $a/f_a = 0$, the pseudoscalar contribution vanishes and the contribution to the constituent mass of the up quark is only from the scalar mass. For $a/f_a = \pi$, the scalar mass almost vanishes, except for the contribution from nonzero current quark mass, whereas the pseudoscalar mass contribution becomes the predominant component of the constituent mass. In particular, we can also see that the first order chiral phase transition is sensitive to the scaled axion

field. Increasing a/f_a decreases the baryon chemical potential of the first-order phase transition. In Fig. 1(b), we show the variations of M_u^s and M_u^p with respect to the scaled axion field a/f_a for several baryon chemical potentials. We can clearly see that M_u^s and M_u^p vary with a/f_a in a periodic manner, with a period of 2π . For $\mu_B \leq 1000$ MeV, spontaneous CP violation is clearly evident when $a/f_a = \pi + 2k\pi$, with M_u^p exhibiting two degenerate solutions that differ only in sign. For $\mu_B = 1100$ MeV, we can see the discontinuous changes in the magnitudes of M_u^s and M_u^p , which are results of the first-order chiral phase transition. For $\mu_B = 1200$ MeV, the restoration of chiral symmetry and CP symmetry leads to small and continuous changes in the magnitudes of M_u^s and M_u^p for different values of a/f_a . In Fig. 1 (c) and (d), we also show the axion effect on the pressure of quark matter. It can be seen that as the scaled axion field a/f_a increases, the first-order phase transition in quark matter moves to the lower baryon chemical potential, resulting the earlier appearance of free quarks, and consequently the equation of state of quark matter becomes stiffer. The normalized pressure given by $P - P(a/f_a = 0)$ have a minimum value at $a/f_a = 0$, which is consistent with the Vafa-Witten theorem [61]. After the restoration of chiral symmetry and CP symmetry, the normalized pressure has a peak at $a/f_a = \pi + 2k\pi$.

Next we discuss the axion effects on hybrid star (matter) with the hadron-quark phase transition based on the NJL model for quark matter with the different scaled axion field a/f_a . It is known that the position of the critical point for the chiral phase transition is sensitive to G_V [44, 62, 63], which was later constrained within $0.5G_S \leq G_V \leq 1.1G_S$ from the relative v_2 splitting between protons and antiprotons as well as between K^+ and K^- in relativistic heavy-ion collisions [64]. Therefore, we fix the coupling constant $G_V = 0.5G_S$, which can allow the maximum mass of the hybrid star to approach $2 M_\odot$. We show in Fig. 2 (a) that the EOSs of hybrid star matter with the hadron-quark phase transition for the different scaled axion field a/f_a . The color cycles in the inset panel denote the onsets of the hadron-quark mixed phases. With increasing a/f_a , the EOS of pure quark phase in hybrid star becomes stiffer, which is consistent with that observed in Fig. 1 (c), whereas the shift of the mixed phase onset to lower densities actually softens the EOS of the mixed phase matter due to the earlier appearance of additional degrees of freedom. Using the EOS with the hadron-quark phase transition, we can determine the other properties of hybrid star matter. In Fig. 2 (b) and (c), we show that the squared speed of sound c_s^2 and the polytropic index γ as functions of the baryon density in hybrid star with the hadron-quark phase transition by varying the scaled axion field a/f_a . The speed of sound and polytropic index are respectively defined as $c_s^2 \equiv \partial P / \partial \varepsilon$ and $\gamma \equiv d(\ln P) / d(\ln \varepsilon)$, which are considered to be good approximate criteria for the evidences of SQM in neutron star [10, 49, 65–67]. As shown in Fig. 2 (b) and (c), we can observe a step-like decrease

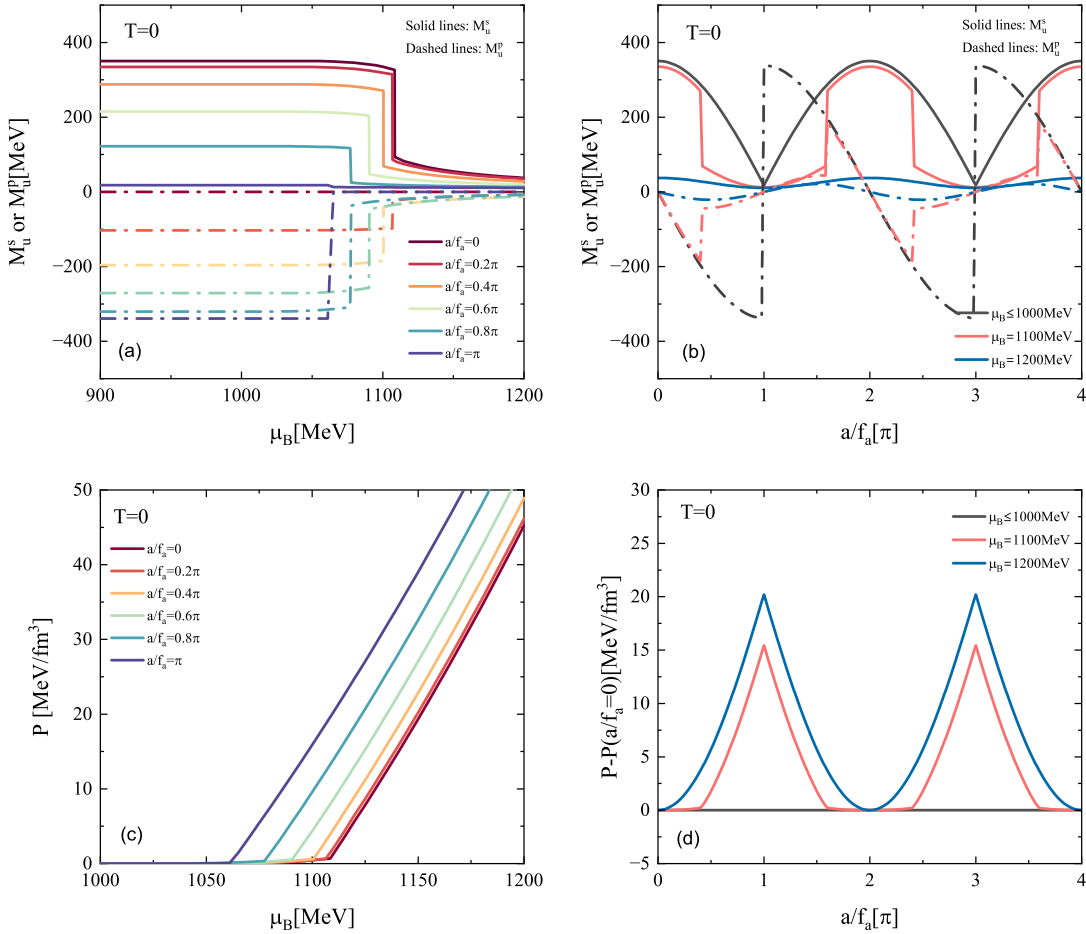


FIG. 1. Axion effects on quark matter at zero temperature from NJL model with $G_V = 0$, including (a) the scalar and pseudoscalar contributions of light quark constituent mass, M_u^s and M_u^p , as functions of the baryon chemical potential for varying values of the scaled axion field a/f_a , (b) M_u^s and M_u^p as functions of the scaled axion field a/f_a for several baryon chemical potentials, (c) pressure as a function of the baryon chemical potential for different values of the scaled axion field a/f_a , and (d) normalized pressure as a function of the scaled axion field a/f_a for different baryon chemical potentials.

in both the speed of sound and the polytropic index during the hadron-quark transition, where the appearance of quarks softens the EOS. Subsequently, these two quantities exhibit another step-like increase as the nucleon and lepton degrees of freedom diminish in the high-density quark phase. It can also be seen that the speed of sound and the polytropic index in the pure quark phase at high densities exceed the conformal limits of $c_s^2 = 1/3$ and $\gamma = 1$, due to the strong repulsive vector interaction in quark matter. Our previous work [49] indicated that if $G_V = 0$, both c_s^2 and γ would converge to the conformal limit. Our results also agree with the approximate rules that $\gamma \leq 1.75$ [10] or $\gamma \leq 1.6$ and $c_s^2 \leq 0.7$ [65] can be used as criteria for distinguishing hadronic matter from quark matter. The scaled axion field has slight impact on the speed of sound and polytropic index in mixed and

pure quark phase, which indicates that after the appearance of quark matter, the effect of axions on the equation of state of hybrid star matter is mostly not dependent on density or energy density.

The mass-radius relation of hybrid star with the scaled axion field is shown in Fig. 2 (d). The constraints from the bayesian analyses of the observational data from the pulsars PSR J0030+0451 [1, 2] and PSR J0740+6620 [4, 5], and from the analyses of the gravitational wave signal from the neutron stars merger GW170817 [6] are shown for comparison. The results indicate that both the observed maximum mass and the corresponding radius of hybrid stars slightly decrease with the increasing a/f_a . This is due to the maximum mass of hybrid stars primarily constraining the EOS of hybrid star matter at densities in the range $2\rho_0 \sim 5\rho_0$, where ρ_0 refers to the

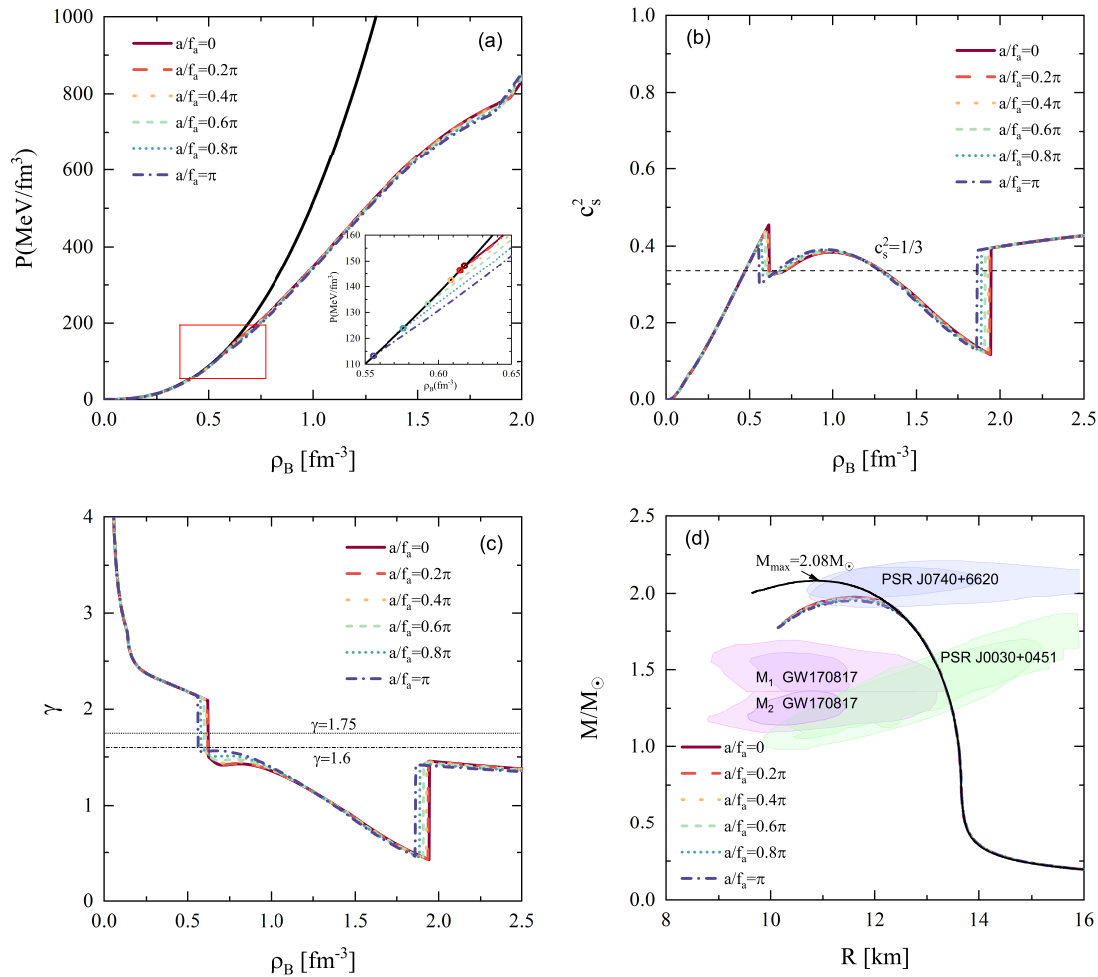


FIG. 2. Axion effects on hybrid star (matter) with the hadron-quark phase transition based on the NJL model for quark matter with $G_V = 0.5G_S$, and varying the scaled axion field a/f_a . The results include (a) pressure as a function of the baryon density, (b) mass-radius relation, (c) the squared of speed of sound c_s^2 as a function of the baryon density, and (d) polytropic index γ as a function of the baryon density. In (a), the color cycles indicate the onsets of the hadron-quark mixed phases, and the black solid line represents pure hadronic matter (PHM), which is also shown for comparison. In (d), constraints from multimessenger astronomy observations [12,13,15–17] are shown by shaded regions, see text for details.

saturation density of 0.16 fm^{-3} . As shown in Fig. 2 (a), the hadron-quark mixed phase in most cases occurs at this density region, and thus the property of mixed phase is an important factor affecting the maximum mass of hybrid stars. We also note that masses and radii of hybrid stars in all parameter sets are mostly consistent with the constraints from the pulsars PSR J0030+0451 and PSR J0740+6620, as well as the neutron star merger GW170817. The hybrid star matter consists of charge-neutral matter in β -equilibrium that has a hadron-quark phase transition from hadronic to quark matter. To better understand the axion effects on quark matter in the hybrid stars, we show in Fig. 3 the radii and masses of quark-matter cores in the maximum-mass hybrid stars for

the different scaled axion field a/f_a . In this work, we consider the quark-matter core including the pure quark phase and the mixed phase. Using the TOV equations, the pressure is integrated from the central baryon density to the onset of the mixed phase to determine the size of quark-matter core. As shown in Fig. 3, although the axion has a minimal impact on the mass and radius of the maximum-mass hybrid star, and even slightly reduces these values as a/f_a increases, it significantly increases the radius and mass of the quark-matter core. This is due to the axion effect substantially lowering the density of onset of the mixed phase, while the central density of the maximum-mass hybrid star remains almost constant for different values of a/f_a . For the case $a/f_a = \pi$,

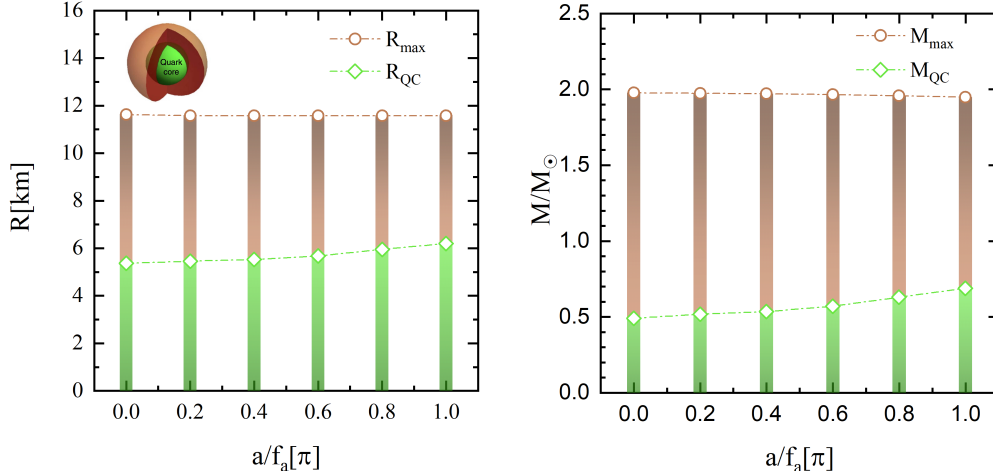


FIG. 3. Radii and masses of quark-matter cores in the maximum-mass hybrid stars for varying values of the scaled axion field a/f_a . The green bars represent the radii and masses of the quark-matter cores, while the chocolate-colored bars represent the radii and masses of the remaining parts.

the mass of the quark-matter core in a hybrid star with nearly $2M_{\odot}$ can reach up to $0.7M_{\odot}$, and the radius of core $R_{\text{QC}} = 6.2$ km exceeds half of the star's total radius. Therefore, our results indicate with axion effects, a sizable quark-matter core can appear in $2M_{\odot}$ massive neutron stars.

Summary and outlook. In this work, we investigate the axion effects on quark matter and quark-matter core in massive hybrid stars with the hadron-quark phase transition based on the three flavor NJL model. Our results indicate within the range of 0 to π for the scaled axion field a/f_a , the scalar contribution of the constituent mass M_u^s decreases as a/f_a increases, while the pseudoscalar contribution M_u^p increases with a/f_a . We also find that the first-order chiral phase transition is sensitive to the axion field. Increasing a/f_a decrease the baryon chemical potential of the first-order phase transition, leading to the earlier appearance of free quarks. Consequently, the equation of state for quark matter becomes stiffer. The effect of axions on hybrid star matter that includes the hadron-quark phase transition is contrary to expectations. The axion field shifts the onset of the mixed phase to lower densities but slightly softens the equation of state of the mixed phase matter, which also results in a slight decrease in the maximum mass and radius of the hybrid stars. However, we note that the lowering of the onset of the mixed phase significantly increases the radius and mass of the quark-matter core in the hybrid star. Therefore, our results indicate with axion effects, a sizable quark-matter core can appear in $2M_{\odot}$ massive neutron stars. As a candidate for cold dark matter, we

expect that the results on axions presented in this paper will complement recent studies on the effects of beyond-the-Standard-Model particles on the structure of NSs and the dynamics of binary NS mergers, and contribute to a deeper understanding of these effects.

In the study of other properties of hybrid star matter, we observe that a step-like decrease in both the speed of sound and the polytropic index during the hadron-quark transition, where the appearance of quarks softens the EOS. A recent research in Ref. [13] suggests that the EOS with a sudden change in the speed of sound can leave a clear and unique signature in the main frequency of the postmerger gravitational wave (GW) spectrum, which provide a sensitive probe of the hadron-quark phase transition in the massive neutron star. Our results also agree with the approximate rules following Refs. [10, 65] that $\gamma \leq 1.75$ and $\gamma \leq 1.6$ and $c_s^2 \leq 0.7$ can be used as criteria for separating hadronic from quark matter. Our previous work [68] indicate the speed of sound and polytropic index can also be used to the search for QCD critical point in heavy-ion collisions. Therefore, we hope to further explore the effects of axion on the QCD phase diagram and critical point through observable quantities such as higher-order fluctuations, speed of sound, and polytropic index.

This work is supported by the National Natural Science Foundation of China under Grants No. 12205158 and No. 11975132, and the Shandong Provincial Natural Science Foundation, China Grants No. ZR2021QA037, No. ZR2022JQ04, No. ZR2019YQ01, and No. ZR2021MA037.

[1] T. E. Riley, A. L. Watts, S. Bogdanov, *et al.* *Astrophys. J. Lett.* **887**, L21, (2019).

[2] M. C. Miller, F. K. Lamb, A. J. Dittmann, *et al.* *Astro-*

- phys. J. Lett. **887**, L24, (2019).
- [3] H. T. Cromartie, E. Fonseca, S. M. Ransom, *et al.* Nature Astronomy, **4**, 72, (2020).
- [4] T. E. Riley, A. L. Watts, P. S. Ray *et al.* Astrophys. J. Lett. **918**, L27, (2021).
- [5] M. C. Miller, F. K. Lamb, A. J. Dittmann *et al.* Astrophys. J. Lett. **918**, L28 (2021).
- [6] B. P. Abbott *et al.* (LIGO Scientific Collaboration Virgo Collaboration), Phys. Rev. Lett. **119**, 161101 (2017).
- [7] B. P. Abbott *et al.* (LIGO Scientific Collaboration Virgo Collaboration), Astrophys. J. Lett. **896**, L44 (2020).
- [8] F. Weber, Prog. Part. Nucl. Phys. **54**, 193 (2005).
- [9] Y. Aoki, G. Endrődi, Z. Fodor, S. D. Katz, and K. K. Szabó, Nature **443**, 675 (2006).
- [10] E. Annala, T. Gorda, and A. Kurkela, J. Nättilä, and A. Vuorinen, Nat. Phys. **16**, 907 (2020).
- [11] M. G. Alford, S. Han, and K. Schwenzer, J. Phys. G **46**, 114001 (2019).
- [12] A. Bauswein, N. F. Bastian, D. B. Blaschke, K. Chatziioannou, J. A. Clark, T. Fischer, and M. Oertel, Phys. Rev. Lett. **122**, 061102 (2019).
- [13] Y. J. Huang, L. Baiotti, T. Kojo, K. Takami, H. Sotani, H. Togashi, T. Hatsuda, S. Nagataki, and Y. Z. Fan, Phys. Rev. Lett. **129**, 181101 (2022).
- [14] A. Hook and J. Huang, J. High Energy Phys. **06**, 036 (2018) .
- [15] J. Zhang, Z. Lyu, J. Huang, M. C. Johnson, L. Sagunski, M. Sakellariadou, and H. Yang, Phys. Rev. Lett. **127**, 161101 (2021).
- [16] P. S. B. Dev, J-F.Fortin, S. P. Harris, K. Sinha, and Y. Zhang, Phys. Rev. Lett. **132**, 101003 (2024)
- [17] M. Diamond, D. Fiorillo, G. Marques-Tavares, I. Tamborra, and E. Vitagliano, Phys. Rev. Lett. **132**, 101004 (2024)
- [18] P. S. B. Dev, J-F. Fortin, S. P. Harris, K. Sinha, and Y. Zhang, J. Cosmol. Astropart. Phys. **01**, 006 (2022).
- [19] M. D. Diamond and G. Marques-Tavares, Phys. Rev. Lett. **128**, 211101 (2022).
- [20] S. Weinberg, Phys. Rev. Lett. **40**, 223 (1978).
- [21] F. Wilczek, Phys. Rev. Lett. **40**, 279 (1978).
- [22] M. S. Turner and F. Wilczek, Phys. Rev. Lett. **66**, 5 (1991).
- [23] D. J. Marsh, Phys. Rep. **643**, 1 (2016).
- [24] G. Raffelt and D. Seckel, Phys. Rev. Lett. **67**, 2605 (1991).
- [25] H.-T. Janka, W. Keil, G. Raffelt, and D. Seckel, Phys. Rev. Lett. **76**, 2621 (1996).
- [26] A. Sedrakian, Phys. Rev. D **93**, 065044 (2016).
- [27] A. Sedrakian, Phys. Rev. D **99**, 043011 (2019).
- [28] S. R. Coleman, Subnuclear series **15**, 805 (1979)
- [29] R. D. Peccei and H. R. Quinn, Phys. Rev. Lett. **38**, 1440 (1977).
- [30] R. D. Peccei and H. R. Quinn, Phys. Rev. D **16**, 1791 (1977).
- [31] D. Boer and J. K. Boomsma, Phys. Rev. D **78**, 054027 (2008)
- [32] B. Chatterjee, H. Mishra, and A. Mishra, Phys. Rev. D **85**, 114008 (2012)
- [33] A. Abhishek, A. Das, R. K. Mohapatra, and H. Mishra, Phys. Rev. D **103**, 074003 (2021)
- [34] G. t' Hooft, Phys. Rev. D **14**, 3432 (1976); **18**, 2199(E) (1978).
- [35] G. G. Raffelt, Lect. Notes Phys. **741**, 51 (2008).
- [36] J. H. Chang, R. Essig, and S. D. McDermott, J. High Energy Phys. **09**, 051 (2018).
- [37] N. Bar, K. Blum, and G. Damico, Phys. Rev. D **101**, 123025 (2020).
- [38] K. Fukushima, Physics Letters B **591**, 277(2004).
- [39] P. Zhuang, J. Huefner, S. P. Klevansky, Nucl. Phys. A **576**, 525 (1994).
- [40] J. K. Boomsma and D. Boër, Phys. Rev. D **80**, 034019 (2009).
- [41] D. Boër and J. K. Boomsma, Phys. Rev. D **78**, 054027 (2008).
- [42] B. Chatterjee and H. Mishra, Phys. Rev. D **85**, 114008 (2012).
- [43] M. Lutz, S. Klimt, W. Weise, Nucl. Phys. A **542**, 521 (1992).
- [44] N. M. Bratovic, T. Hatsuda, W. Weise, Phys. Lett. B **719**, 131 (2013).
- [45] E. Farhi and R. L. Jaffe, Phys. Rev. D **30**, 2379 (1984).
- [46] E. Witten, Phys. Rev. D **30**, 272 (1984).
- [47] J. Xu, L. W. Chen, and B. A. Li, Phys. Rev. C **91**, 014611 (2015).
- [48] H. Liu, J. Xu, and P. C. Chu, Phys. Rev. D **105**, 043015 (2022).
- [49] H. Liu, X. M. Zhang, and P. C. Chu, Phys. Rev. D **107**, 094032 (2023).
- [50] A. Carbone, A. Rios, and A. Polls, Phys. Rev. C **90**, 054322 (2014).
- [51] A. Carbone, A. Polls, and A. Rios, Phys. Rev. C **98**, 025804 (2018).
- [52] C. Wellenhofer, J. W. Holt, and N. Kaiser, Phys. Rev. C **92**, 015801 (2015).
- [53] C. Wellenhofer, J. W. Holt, and N. Kaiser, Phys. Rev. C **93**, 055802 (2016).
- [54] N. K. Glendenning, Phys. Rep. **342**, 393 (2001).
- [55] N. K. Glendenning, Phys. Rev. D **46**, 1274 (1992).
- [56] J. Xu, L. W. Chen, B. A. Li, and H. R. Ma, Phys. Rev. C **79**, 035802 (2009).
- [57] J. Xu, L. W. Chen, B. A. Li, and H. R. Ma, Astrophys. J. **697**, 1549 (2009).
- [58] J. Carriere, C. J. Horowitz, and J. Piekarewicz, Astrophys. J. **593**, 463 (2003).
- [59] G. Baym, C. Pethick, and P. Sutherland, Astrophys. J. **170**, 299 (1971).
- [60] J. Oppenheimer and G. Volkoff, Phys. Rev. **55**, 374 (1939).
- [61] C. Vafa and E. Witten, Phys. Rev. Lett. **53**, 535 (1984).
- [62] M. Asakawa and K. Yazaki, Nucl. Phys. A **504**, 668 (1989).
- [63] K. Fukushima, Phys. Rev. D **77**, 114028 (2008); **78**, 039902 (E) (2008).
- [64] J. Xu, T. Song, C. M. Ko, and F. Li, Phys. Rev. Lett. **112**, 012301 (2014).
- [65] M. Z. Han, Y. J. Huang, S. P. Tang, and Y. Z. Fan, Sci. Bull. **68**, 913 (2023).
- [66] H. Liu, Y. H. Yang, Y. Han, and P. C. Chu, Phys. Rev. D **108**, 034004 (2023).
- [67] Y. H. Yang, H. Liu, P.C. Chu, Nucl. Sci. Tech. **35**, 166 (2024).
- [68] H. Liu, Y. H. Yang, C. Yuan, M. Ju, X. H. Wu, and P. C. Chu, Phys. Rev. D **109**, 074037 (2024).